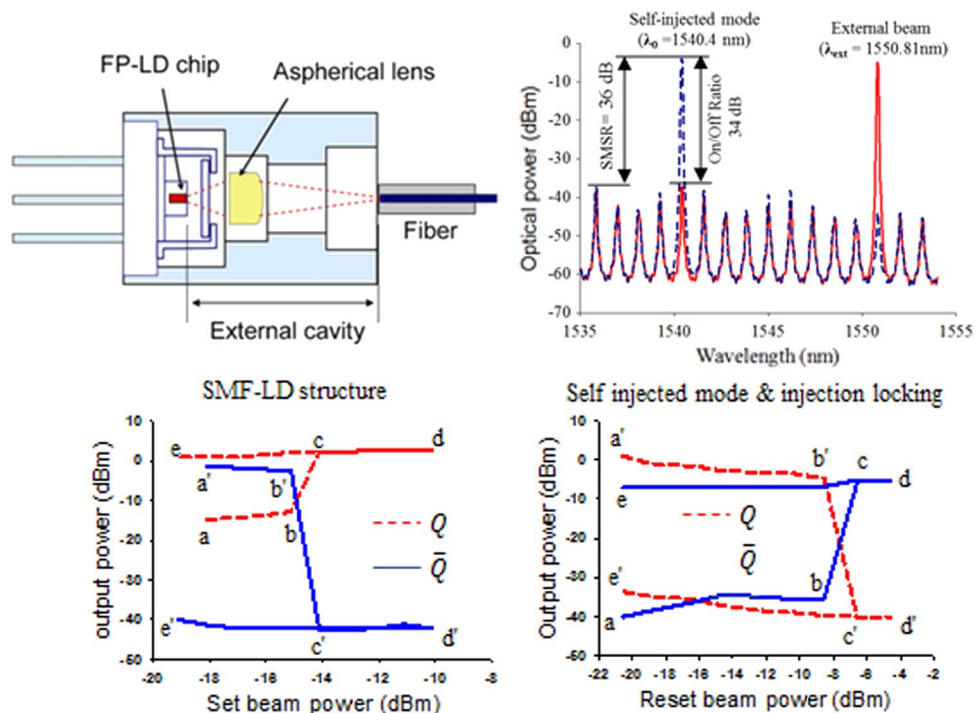


# Analysis of Hysteresis Width on Optical Bistability for the Realization of Optical SR Flip-Flop Using SMFP-LDs With Simultaneous Inverted and Non-Inverted Outputs

Volume 6, Number 3, June 2014

B. Nakarmi  
T. Q. Hoai  
Y. H. Won  
Xuping Zhang



DOI: 10.1109/JPHOT.2014.2323303  
1943-0655 © 2014 IEEE

# Analysis of Hysteresis Width on Optical Bistability for the Realization of Optical SR Flip-Flop Using SMFP-LDs With Simultaneous Inverted and Non-Inverted Outputs

B. Nakarmi,<sup>1,2</sup> T. Q. Hoai,<sup>3</sup> Y. H. Won,<sup>2,3</sup> and Xuping Zhang<sup>1</sup>

<sup>1</sup>Institute of Optical Communication Engineering, Nanjing University, Nanjing 210093, China

<sup>2</sup>Department of Electrical Engineering, Korea Advanced Institute of Science and Technology, Daejeon 305-701, Korea

<sup>3</sup>Information and Communication Engineering, Korea Advanced Institute of Science and Technology, Daejeon 305-701, Korea

DOI: 10.1109/JPHOT.2014.2323303

1943-0655 © 2014 IEEE. Translations and content mining are permitted for academic research only. Personal use is also permitted, but republication/redistribution requires IEEE permission.

See [http://www.ieee.org/publications\\_standards/publications/rights/index.html](http://www.ieee.org/publications_standards/publications/rights/index.html) for more information.

Manuscript received March 26, 2014; revised April 28, 2014; accepted May 2, 2014. Date of publication May 13, 2014; date of current version May 29, 2014. This work was supported in part by the Korea Advanced Institute of Science and Technology through the BK21 Program, by the National Natural Science Foundation of China under Grant 61027017, and by the National Basic Research Program of China (973 Program) under Grant 2010CB327803. Corresponding author: B. Nakarmi (e-mail: bikash@kaist.ac.kr).

**Abstract:** The width of hysteresis in optical bistability plays an important role on latching operation. The injected input optical power and wavelength detuning in single mode Fabry–Perot laser diode (SMFP-LD) are two parameters that can impact the width of hysteresis in bistability of dominant mode and injected mode. In this paper, we analyze the effect of wavelength detuning on width of the hysteresis loop, the dynamic power range for optical bistability, and the rising–falling time of output waveform. With this analysis, optical Set Reset flip-flop with simultaneous inverted and non-inverted output at the data rate of 8.5 Gb/s are obtained using SMFP-LDs. The principle is based on the optical bistability phenomena during injection-locking of the Fabry–Perot laser diode. The set and reset pulses are maintained in low power of about  $-14$  and  $-6$  dBm for the power effective configuration. The contrast ratios of more than 20 dB with simultaneous non-inverted and inverted output Q and  $\bar{Q}$  are observed. Clear output spectrum domain results, waveforms, eye diagram with extinction ratio of more than 12 dB, a rising/falling time of about 40 ps, and bit error rate (BER) measurement without noise floor up to  $10^{-12}$  are observed. The maximum power penalty is about 1.8 dB at BER of  $10^{-9}$ .

**Index Terms:** Hysteresis loop width, Fabry–Perot laser diode, injection locking, SR Latch.

## 1. Introduction

The present state research and development in optical signal processing has made possible of increasing data rates to gigabits per second and terabits per second per fiber [1]. Among various optical units, optical flip-flops (OFFs) contribute significantly in optical signal processing [2]. OFFs can be used for the storage of packet header information, building blocks for shift registers, counters, regenerative memory circuit and many other [3]–[6]. In literature, several optical components

such as coupled ring and array wave guide [7], Mach–Zehnder interferometers (MZIs) [8], [9], non-linear polarization switches [10] and ordinary commercially available Fabry–Perot laser diodes (FP-LDs) [11] are used to demonstrate OFFs. OFFs using coupled ring lasers and array waveguide with each ring laser having a separate gain element, semiconductor optical amplifier (SOA), are based on the gain quenching concept and have constraints on speed limitation due to the cavity length of about 4.5 mm. Significant work has been done in OFFs using SOAs by many research groups [12]–[14] as it has advantages of integrability and high data rates, but SOAs need high driving current of more than 200 mA, are expensive, and require an additional probe beam. The requirement of probe beam further increases the system cost, power requirement, and complexity in structure. FP-LDs require less current, and are of low cost but still require an additional probe beam for the operation. OFFs realization using FP-LDs in [11] shows low ON/OFF contrast ratio, only one output port of OFF, and also low data rate of 1 Gbps. The need of an additional probe beam and low ON/OFF contrast ratio can be overcome by using a SMFP-LD which has a single dominant mode with high side mode suppression ratio (SMSR) in contrast to commercially available ordinary FP-LD [15]. In SMFP-LD, the power difference between the dominant self-injected mode and the corresponding side mode are high, and hence, the high ON/OFF contrast ratio with injection and normal condition can be obtained with the use of SMFP-LDs for optical SR flip-flop. The innate properties of SMFP-LD which has the average biasing current of about 15 mA, is cheap and does not need any probe beam as required in ordinary FP-LD and other optical technologies, makes it a better candidate for optical signal processing in the future.

Optical bistability phenomena in FP-LD have been analyzed in number of literatures [16]–[18] and had performed theoretical analysis on the hysteresis width of optical bistability with side mode suppression ratio, switching time and energy on the optical bistability of multi-mode FP-LDs. In this paper, we analyze experimentally the hysteresis width, and rising/falling time of the output of optical bistability in external cavity based SMFP-LD. The experimental results of change in hysteresis width due to wavelength detuning match with the theoretical analysis performed in [17]. However, they used conventional FP-LDs for the analysis. SMFP-LDs and conventional FP-LDs are similar in operation except the former has only one dominant mode and all other side modes are suppressed on normal operating condition, whereas the latter has many side modes with less contrast on power of side modes with respect to the corresponding near modes. With the analysis of hysteresis width and rising/falling time of output due to change in wavelength detuning on SMFP-LD, we propose and demonstrate simultaneous non-inverted and inverted SR flip-flop using SMFP-LDs. In the proposed scheme, two SMFP-LDs are used with a feedback of one to another making it sequential circuit. As one of the main advantages of SMFP-LD is the power effective approach, we have set the optical set and reset pulses to low power of  $-14$  dBm and  $-6$  dBm, respectively. With this power, we obtained clear output waveforms, rising/falling time of about 30 ps and 40 ps, respectively, and clear eye diagrams with extinction ratio of more than 12 dB. No noise floor is seen up to BER of  $10^{-12}$  for both Q and  $\bar{Q}$  output, and maximum power penalty of 1.8 dB is measured at the BER of  $10^{-9}$ .

## 2. Working Principle and Analysis

The FP-LD used in this experiment is a specially designed FP-LD in our lab which has a self-injected dominant mode with high suppression ratio [15]. The SMFP-LD is obtained by eliminating the inclination of  $6^\circ$  to  $8^\circ$ , present in the conventional FP-LDs of the coupling fiber thereby forming an external cavity between laser diode and the fiber. The SMFP-LD consists of a FP-LD chip with an InGaAsP multi-quantum well structure of  $300\ \mu\text{m}$  and an external cavity length of 4 mm, and it operates in a single longitudinal mode. By varying the temperature, the mode matching condition is achieved for both of the cavities. With changes in temperature, the refractive index of the active region changes and hence there is a change in optical path length in the laser diode which provides optimal mode matching condition for the single mode oscillation. Single mode oscillation can be tuned to another adjacent mode which gives the tunability of SMFP-LDs by varying the operating temperature. The self-locking mode of SMFP-LD is tunable for a wide range of wavelengths of 10 nm

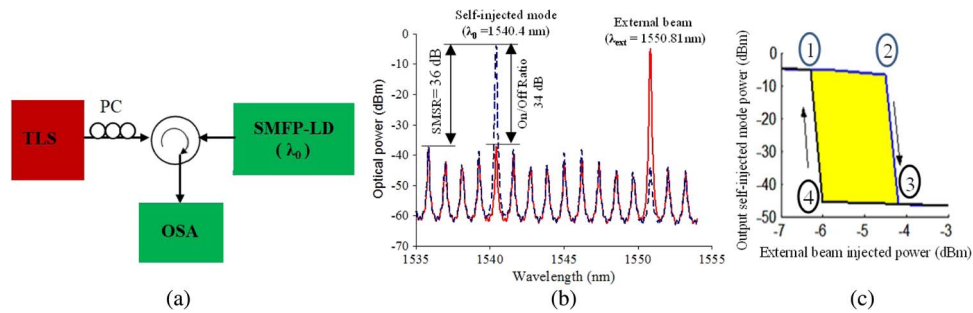


Fig. 1. Optical bistability in SMFP-LD. (a) Block diagram for observing optical bistability and rising falling time at output. (b) Self injected beam of SMFP-LD and injection locking. (c) Optical bistability illustration with self-injected mode power versus injected beam power.

by adjusting the operating temperature. We have used the commercially available thermal electric cooler which has the temperature sensitivity of less than  $0.01\text{ }^{\circ}\text{C}$  for the temperature stability in SMFP-LD operation. The SMFP-LD is equivalent to conventional FP-LD with the injection of external beam. The operation of proposed simultaneous output SR Flip-Flop is based on the bistability property of injection locking on SMFP-LD. Injection locking refers to the state when the dominant self-injected beam is suppressed sufficiently with the injection of the external beam which can be obtained by proper wavelength detuning and input injected power selection [19]. During the injection locking, bistability occurs which shows two stable conditions based on the state of input beams. The bistability property in SMFP-LD is due to the power difference between the power needed by the injected beam for suppressing the dominant mode and the power needed for releasing the dominant mode back to the unlocked mode. Since the power needed for the injection locking for the suppression of the self-injected mode in SMFP-LD is dependent on the wavelength detuning, the bistability in SMFP-LD also depends on the injected beam power and wavelength detuning. The effect of wavelength detuning on the stability of injection locking with a single injected mode has been analyzed in [20] and it is shown that the negative wavelength detuning will result in unstable locking regime. However, with more than single injected locked modes, the negative wavelength detuning has relatively small region of instability but the negative wavelength detuning cannot provide the bistability [21]. Hence, we have only considered the effect of positive wavelength detuning on hysteresis width in optical bistability and rising/falling time of output ports.

Fig. 1 illustrates the injection locking and bistability phenomena in SMFP-LD. Fig. 1(a) shows the block diagram used to observe the injection locking and optical bistability in SMFP-LD. The SMFP-LD used in the experiment has a dominant self-injected mode at the wavelength of  $\lambda_0$ . Tunable laser source (TLS) is used to vary the wavelength and power of injected external beam  $\lambda_{ext}$  as shown in Fig. 1(a). With the driving current of 15 mA and temperature of  $21\text{ }^{\circ}\text{C}$ , SMFP-LD is self-locked at the dominant mode of 1540.4 nm with side mode suppression ratio (SMSR) of about 36 dB. When the external beam from TLS is injected to SMFP-LD with the wavelength detuning of 0.12 nm with sufficient power, the self-injected mode is suppressed as shown in Fig. 1(b) with ON/OFF contrast ratio of about 34 dB. The bistability process is observed when the injected beam power is reduced after the injection locking process with the suppression of dominant mode. While reducing the injected beam power, dominant mode of SMFP-LD will still stay in suppressed mode until the injected beam power reaches to certain value which releases the suppression of dominant mode. In order to observe the bistability phenomenon, we fix wavelength detuning of 0.12 nm and the injected power of external beam is slowly varied. The position 1 in Fig. 1(c) denotes the starting point without any suppression of the self-injected mode of the SMFP-LD. On increasing the power of injected beam, no significant suppression occurs unless the injected power reaches to  $-4.2\text{ dBm}$  (position 2). Beyond the power of  $-4.2\text{ dBm}$ , the self-injected mode of SMFP-LD is suppressed significantly (shift position 2 to position 3) with the suppression ratio of about 40 dB. On increasing the power, the dominant mode will keep on suppressing but on reducing the power the self-injected mode does not return back to the unlocked position 2 or 1, even when the power is less than

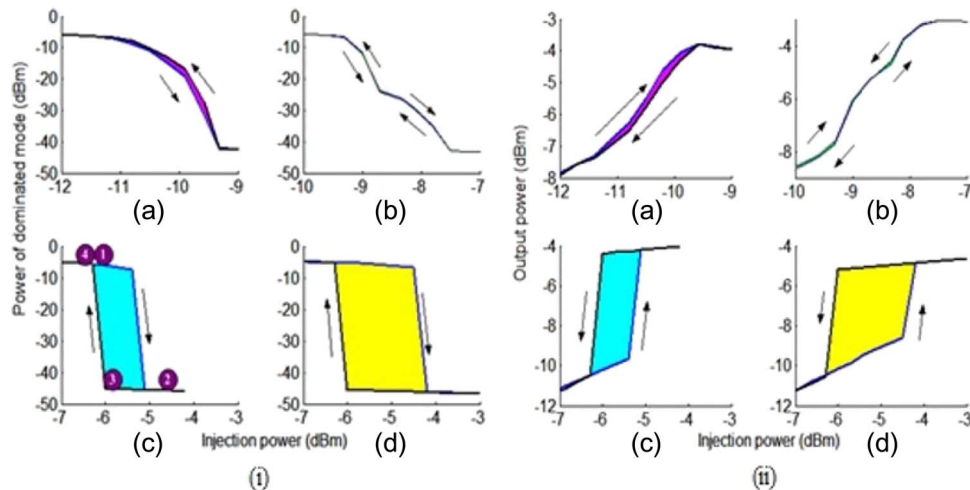


Fig. 2. Hysteresis curves of the (i) dominated mode and (ii) injected mode against the various wavelength detuning. (a) 0.02 nm, (b) 0.04nm, (c) 0.08 nm, and (d) 0.12 nm.

−4.2 dBm, which is the initial power required for the suppression. The self-injected mode is unlocked and will gain the same power as that of the unlocked state returning to position 1, only when the power of external injected beam is reduced to −6.1 dBm. This completes the hysteresis loop of optical bistability of the dominant mode in SMFP-LD.

To find the effect of change in wavelength detuning in optical bistability, we analyze the hysteresis loop with different wavelength detuning. The notable observation made during this process is the change in the width of the hysteresis. Fig. 2(i) shows the corresponding hysteresis curve of the dominant mode as a function of injection power with different wavelength detuning. Fig. 2(i)-(a) and (i)-(b) shows the hysteresis curve with wavelength detuning of 0.02 nm and 0.04 nm. We can see that the hysteresis loop width is small in both cases and the dominant mode power drops sharply compared to that of Fig. 2(i)-(c) and (i)-(d) which has higher wavelength detuning. In addition, some noticeable issues are counterclockwise hysteresis with detuning of 0.02 nm, and a butterfly hysteresis loop with the increases in detuning to 0.04 nm. In Fig. 2(i)-(c), the wavelength detuning is maintained at 0.08 nm. When the injected power is set initially to a value of −6 dBm (marker 1), the power of the dominant mode is about −5 dBm level. However, when the injected power is increased to −5.1 dBm, the dominant mode is fully suppressed. On the contrary, when the injected beam power decreases below −5.1 dBm after the injection locking with suppression of dominant mode, the output of dominant mode still has low output state (state of marker 2 and 3). The dominant mode will remain suppressed until the input injected beam is higher than −6.2 dBm. To change the dominant mode back to its high output state, the injected power is slightly decreased from −6.2 dBm (marker 4), which returns the dominant mode to the unsuppressed mode and back to initial state (marker 1 again). This process completes the hysteresis loop. From Fig. 2, it is seen that the corresponding modulation depth (value of high-output to low-output states) can reach up to 40 dB. In addition, when the wavelength detuning is increased to 0.12 nm, the hysteresis loop width is further extended, which is illustrated in Fig. 2(i)-(d). It is noted that the optical bistability shown in Fig. 2(i) exhibits a transition from counterclockwise to clockwise hysteresis through a butterfly hysteresis when the detuning is increased from 0.02 nm to 0.12 nm. The injected mode also shows the optical bistability phenomenon as illustrated in Fig. 2(ii) but the hysteresis direction is reversed under the condition of same detuning, and also the obtained optical modulation depth is less than 10 dB.

Fig. 3 illustrates the effect of wavelength detuning on rising/falling time at the output taken at the wavelength of  $\lambda_1 = \lambda_s$ . We measure the output of the SMFP-LD with a 10 Gb/s non return to zero (NRZ) input signal. From the experimental result presented in Fig. 3, the falling time is higher than that of the rising time. It is due to the presence of  $\lambda_1$  at SMFP-LD2 which is used for the weak



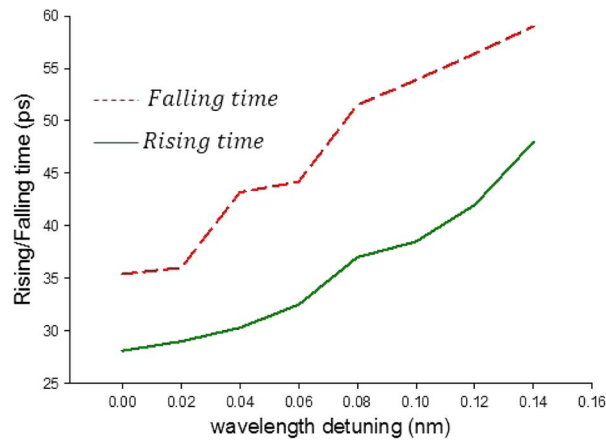


Fig. 3. Effect of wavelength detuning on rising/falling time of output.

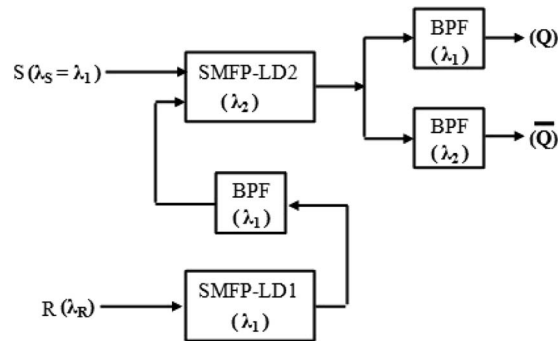


Fig. 4. Block diagram of simultaneous inverted and non-inverted SR flip-flop.

injection locked at the mode of  $\lambda_s$  wavelength. Also, with increase of the wavelength detuning, the rising and falling time increases which is due to the increase in power requirement for suppression of dominant mode by the input signal and the increase in the hysteresis width. From this analysis and result of hysteresis width and rising and falling time, we can clearly ascertain that the injection locking in SMFP-LD with small wavelength detuning such as 0.02 nm is good for the high speed switching and control circuit. With lower detuning range, the recovery time from the suppression of the dominant mode to the original gain of dominant mode is lesser. On the other hand, higher wavelength detuning such as 0.12 nm can be utilized for optical memory and flip-flop applications due to the wider width of the hysteresis loop.

The optical bistability phenomena present in the injection locking process is the basic phenomenon for the realization of SR flip-flop is shown in Fig. 4. For the set state of the SR flip-flop, the set signal S is set to 1 and reset signal R to 0. The power at the wavelength  $\lambda_1$  (total power from S beam and dominant mode of SMFP-LD1) is enough to suppress the dominant mode of SMFP-LD2 forcing  $\bar{Q}$  into logic 0 and Q into logic 1. In order to maintain the output of SR flip-flop in the same state even when the set signal is 0, the self-injected mode should be kept at the suppressed state. Hence, the power of the self-injected mode of SMFP-LD1 should be higher than the unlocked power and lesser than the power required for the injection locking with suppression as shown in Fig. 1(c). This verifies the set condition of optical SR flip-flop. For the reset condition, the reset beam R is made logic 1 and S as logic 0, so that the self-injected mode of SMFP-LD1 is suppressed and SMFP-LD2 is not injection-locked. Hence, the output of Q and  $\bar{Q}$  will be logic 0 and logic 1, respectively. In this case even after the reset signal is removed the output will be the same because when the reset signal is removed, the self-injected mode of the SMFP-LD2 will not be suppressed

TABLE 1

SR flip-flop truth table

Set	Reset	Q	$\bar{Q}$	State
1	0	1	0	Set
0	0	1	0	Set
0	1	0	1	Reset
0	0	0	1	Reset

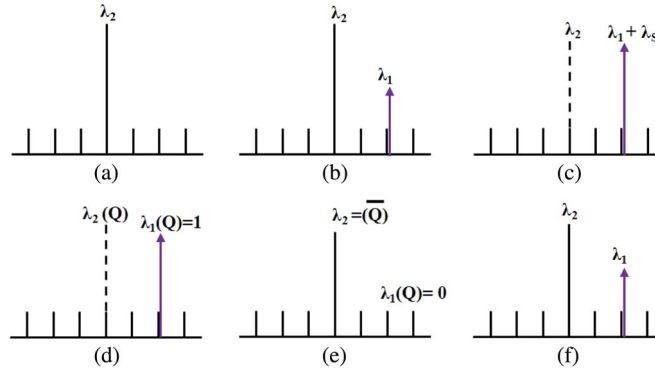


Fig. 5. Spectrum schematic of simultaneous inverted and non-inverted SR flip-flop. (a) Self-injected mode of SMFP-LD2 spectra. (b) SMFP-LD2 spectra with  $\lambda_1$  injection. (c) SMFP-LD2 spectra with  $\lambda_1$  in addition to  $\lambda_s$ . (d) SMFP-LD2 spectra with removal of  $\lambda_s$ . (e) SMFP-LD2 spectra with  $\lambda_R$  injection. (f) SMFP-LD2 spectra with removal of  $\lambda_R$ .

as the power of self-injected mode of SMFP-LD1 alone is not sufficient to suppress the dominant mode of SMFP-LD2. To suppress the self-injected mode of the SMFP-LD2, both the self-injected mode  $\lambda_1$  and set signal  $\lambda_s$  should be logic 1. Thus the truth table of SR flip-flop shown in Table 1 is verified.

The operation of SR flip flop can be further clarified with the spectrum schematic as shown in Fig. 5. Fig. 5(a) shows the spectrum schematic of SMFP-LD2 with the self-injected mode at the wavelength of  $\lambda_2$  in normal condition without any external beam. Fig. 5(b) shows the spectrum schematic with the dominant mode of SMFP-LD1 injected to SMFP-LD2. Since SMFP-LD1 is not injected with any external beam, i.e.,  $R(\lambda_R)$  is logic 0, the self-injected mode of SMFP-LD1,  $\lambda_1$ , will be present in Fig. 5(b). The power of  $\lambda_1$  is maintained in such a way that the power of  $\lambda_1$  alone cannot suppress the self-injected mode  $\lambda_2$  but is sufficient enough to maintain the injection-locked state. Hence,  $\lambda_2$  is not suppressed in Fig. 5(b). When the set beam,  $\lambda_s$ , which is the same wavelength as that of self-injected mode of SMFP-LD1, i.e.,  $\lambda_s = \lambda_1$ , is injected, the self-injected mode of SMFP-LD2,  $\lambda_2$ , is suppressed. It is because the power injected to the SMFP-LD2 (i.e., the combination of  $\lambda_s$  and  $\lambda_1$ ) will be equal or greater than the power required for the suppression of  $\lambda_2$  which is illustrated in Fig. 5(c). After this, even though the set beam is removed and set to  $S = 0$ , the SMFP-LD2 outputs maintain the same state with  $\lambda_2$  suppressed as the power of  $\lambda_1$  is sufficient to hold the same state due to hysteresis curve as shown in Fig. 1(c). This state is schematically shown in Fig. 5(d).

For the reset state, the reset signal  $\lambda_R$  is set to logic 1, which suppresses the dominant mode of SMFP-LD1,  $\lambda_1$ , and hence no beam is injected to SMFP-LD2. In this state the output from the SMFP-LD2 will be the self-injected mode of SMFP-LD2,  $\lambda_2$ . Hence, the output at Q will be logic 0 as Q output is obtained after the signal is filtered by the bandpass filter (BPF) which only passes the wavelength at  $\lambda_1$  but  $\bar{Q}$  will be logic 1 as it is obtained after the beam passing through the BPF

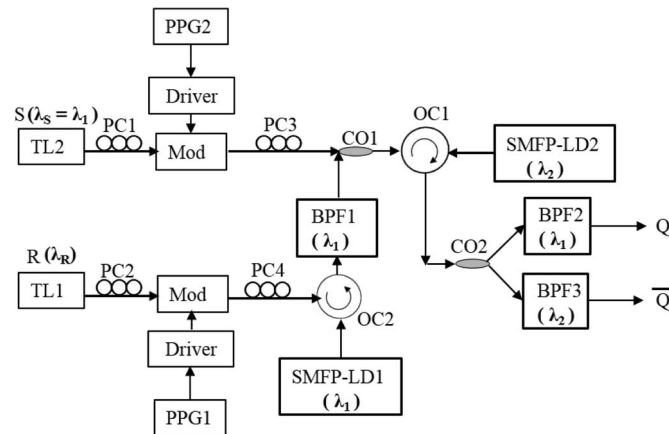


Fig. 6. Experimental set-up for the SR flip-flop with simultaneous inverted and non-inverted outputs. TL: Tunable laser; PC: Polarization controller; PPG: Pulse pattern generator; Mod: Modulator; OC: Optical circulator, Co: coupler; BPF: Band pass filter.

which is tuned at the wavelength of  $\lambda_2$  [shown in Fig. 5(e)]. Again, even though the reset signal is removed, the output ports maintain the same state giving Q as logic 0 and  $\bar{Q}$  as logic 1 since  $\lambda_1$  alone cannot suppress the self-injected mode of the SMFP-LD2,  $\lambda_2$ , which is shown in Fig. 4(f). The schematic spectrum diagram proves that SR latch requires S and R beam to set and reset the latch but does not require the beam to be present to be in the same output state after it is set or reset by S or R beam, respectively.

### 3. Experimental Setup and Results

The experimental set up for the proposed SR flip-flop with simultaneous inverted and non-inverted output is shown in Fig. 6. The proposed scheme uses two self-locked SMFP-LDs among which one is given with a set signal (S) and another with the reset signal (R). SMFP-LD1 and SMFP-LD2 have the self-injected mode at the wavelength of  $\lambda_1$ , 1546.86 nm, and  $\lambda_2$ , 1541.21 nm, when they are biased with the biasing current of 14 mA and 17 mA and the operating temperature of 21 °C and 23.5 °C, respectively. Under these conditions, SMFP-LD1 and SMFP-LD2 have the single mode suppression ratio (SMSR) of about 38 dB and 29 dB, respectively. The output of SMFP-LD1 is feedback to the input of SMFP-LD2 which makes the circuit operate as a sequential circuit. It is noted that the set signal (S), injected to SMFP-LD2 with tunable laser TL2 is in the same wavelength as that of self-injected mode of SMFP-LD1. The reset signal is given as an input for SMFP-LD1 which suppresses the dominant mode of SMFP-LD1  $\lambda_1$  when R signal is logic 1 and will not suppress when there is no input reset beam, R. During the experiment of SR flip-flop, we found that with 0.12 nm wavelength detuning, the minimum power needed to suppress the dominant mode is about -9 dBm (measured after coupler) and the minimum power required to maintain in the same state of the dominant mode is about -12 dBm. Hence, the self-injected mode of SMFP-LD1 should be less than -9 dBm but higher than -12 dBm. Set beam  $\lambda_S$  is configured with less amount of power for  $\lambda_S$  which suppresses the dominant mode of SMFP-LD2 in the presence of  $\lambda_1$  beam. In the experiment, the set beam is applied with the power of -14 dBm. The reset signal is injected at the wavelength of 1550.48 nm with the power of -6 dBm which is sufficient enough to suppress the self-injected mode of SMFP-LD1 alone.

Pulse pattern generators (PPG), PPG1 and PPG 2 generate 8.5 Gb/s NRZ data sequences which are modulated by TL1 and TL2, respectively. Polarization controllers (PC), PC1 and PC2 are used to minimize the loss in the polarization dependent Mach-Zehnder modulator whereas other PCs are used to allow only transverse electric (TE) mode to SMFP-LDs. With transverse magnetic (TM) mode of input beams, FP-LD shows the behavior of the absorption modulation which can be used for the demonstration of the positive logic output, i.e., absorption modulation gives the output contrary to that of injection locking. But in absorption modulation, in addition to the external beam,



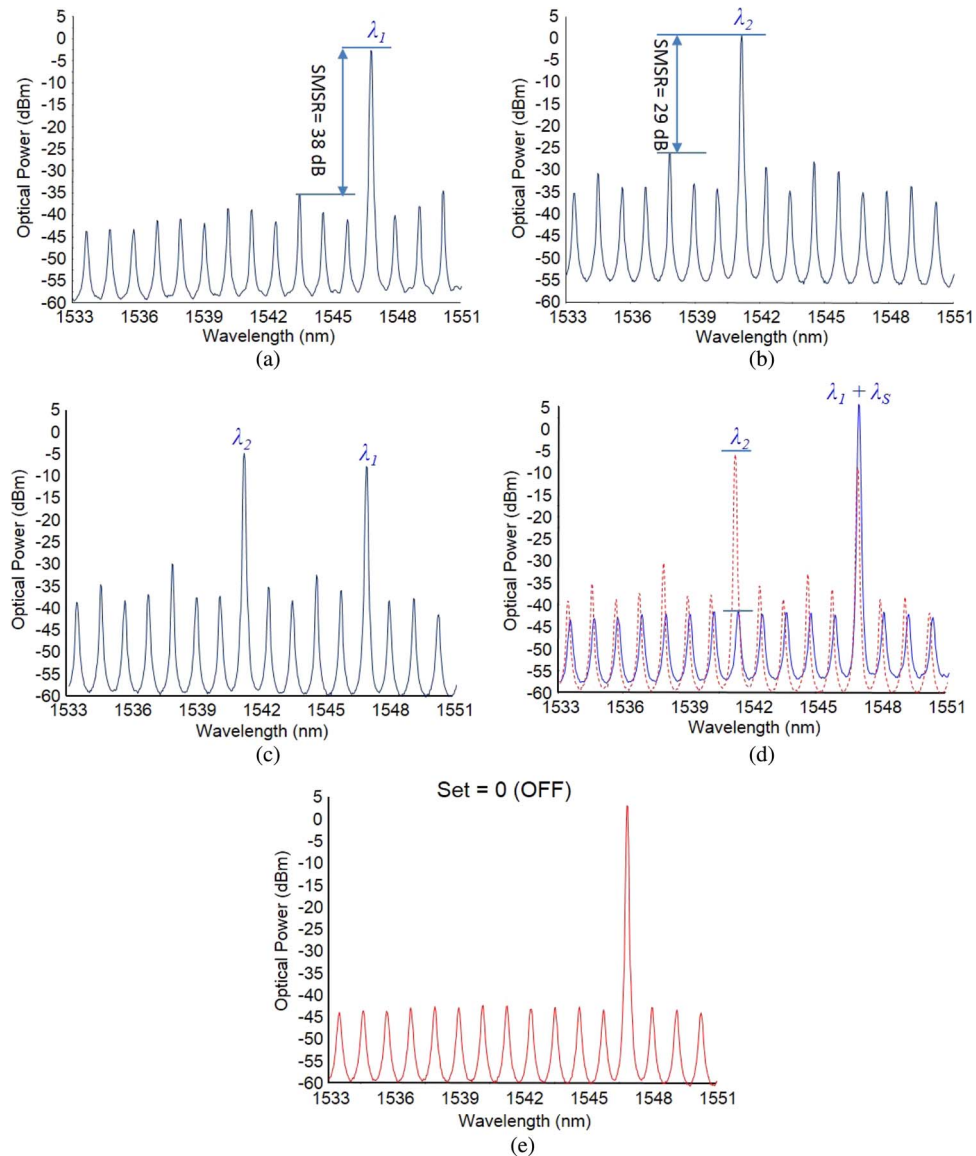


Fig. 7. Spectrum diagram for the set state of proposed SR flip-flop. (a) Dominant mode of SMFP-LD1, (b) dominant mode of SMFP-LD2, (c) SMFP-LD2 is injected with the dominant mode of SMFP-LD1, (d) set state when  $S = 1$ , and (e) output after the removal of  $S$  beam showing output in the same set state.

polarization-sensitive polarization beam splitter is also needed to separate TE- and TM-polarized light, which is expensive [22]. Moreover, in absorption modulation higher data rate performance above 2.5 Gb/s is still not observed which can be easily obtained using injection locking technique. Hence, absorption modulation is not preferred compared to injection locking due to system cost and its complexity on the structure. BPFs are used to filter the beams with desired output wavelengths.

The spectrum domain result for the set state ( $Q = 1$ ) of the proposed flip-flop is shown in Fig. 7. Fig. 7(a) and (b) shows the spectrum diagram of SMFP-LD1 and SMFP-LD2 with dominant mode at  $\lambda_1$ , 1546.86 nm, and  $\lambda_2$ , 1541.21 nm with SMSR of 38 dB and 29 dB, respectively. With  $S = 0$  and  $R = 0$ , the dominant mode of SMFP-LD1 ( $\lambda_1$ ) is passed through the BPF1 and injected to SMFP-LD2. The injected power (power of  $\lambda_1$ ) to SMFP-LD2 is less than  $-9$  dBm, as a result only  $\lambda_1$  cannot suppress the dominant mode of SMFP-LD2 but the power injected at the wavelength of  $\lambda_1$  is

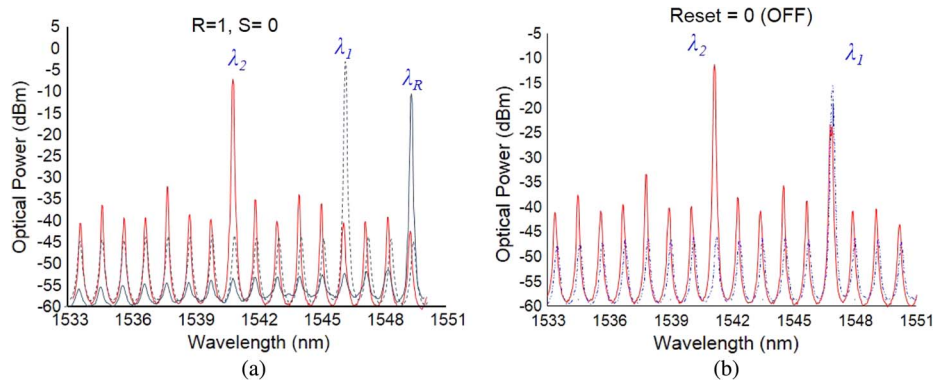


Fig. 8. Spectrum diagram for the reset state of proposed SR flip-flop when (a)  $R = 1$  and  $S = 0$  and (b) when  $R = 0$  and  $S = 0$  after the reset condition.

sufficient enough for injection locking the corresponding mode of SMFP-LD2 as shown in Fig. 7(c). When  $S = 1$ , which is on the same wavelength as that of the dominant mode of SMFP-LD1, the power gained by the beam at the wavelength  $\lambda_1$ , is sufficient enough to suppress the dominant mode of SMFP-LD2 and the combined power with  $S = 1$  and the dominant mode of SMFP-LD1 is recorded as  $-4.2$  dBm. Since BPF2 is tuned at the wavelength of beam S which is also the dominant mode of SMFP-LD1, the output port Q will give the logic 1 output and the output port  $\bar{Q}$  will give logic 0 output as shown in Fig. 7(d). The SR flip-flop remains in the same set state with logic 1 at the output port Q even when the set beam is removed as shown in Fig. 7(e). In this case, the status of S and R are 0 and the past status of S and R as 1 and 0. This is due to the bistability property of injection locking on SMFP-LD. In order to maintain outputs in the same state the power difference between  $S = 1$  and  $S = 0$  should be less than 4 dB which is the dynamic range of power for staying in the locked stage and maintaining the same state without the set beam S. The dynamic range can be made more than 4 dB by increasing the wavelength detuning between the set pulse and the mode of injection at the SMFP-LD as shown in Fig. 2 and increasing the set beam power. It shows that the hysteresis width increases with increase in the wavelength detuning which gives higher dynamic power range.

Fig. 8 shows the spectrum result for the reset state of SR flip flop i.e.,  $\bar{Q}$  will be logic 1 and Q will be logic 0. When reset beam R is logic 1, the dominant mode of SMFP-LD1,  $\lambda_1$ , will be suppressed. In reset state, the set beam is also logic 0. This gives output Q as logic 0 since the output Q is obtained after passing the signal through the BPF1 tuned at the wavelength of  $\lambda_1$ . The output at  $\bar{Q}$  will be logic 1 because there is no injected beam on SMFP-LD2 providing the dominant mode at the wavelength of  $\lambda_2$  as output. This state is illustrated in Fig. 8(a). Similarly as in set state, the reset state will keep the same state even when the reset signal is set to logic 0 due to bistability property which gives the  $\bar{Q}$  as logic 1. In this case Q is logic 0. Spectrum diagrams of Figs. 7 and 8 prove both set and reset state condition for the proposed simultaneous inverted and non-inverted output SR flip-flop using SMFP-LDs as stated in Table 1. The power of Q and  $\bar{Q}$  output of SR flip flop are shown in Fig. 9, which shows the contrast ratio for Q at the set state is less among all other condition and is about 20 dB. Less contrast ratio is due to the fact that the wavelength of set beam is chosen to be the same as the wavelength of dominant mode of SMFP-LD1. The same wavelength of set beam and dominant mode beam is used in order to make SR flip flop with less set signal power.

The output waveform, rising/falling time and eye diagram result for the proposed SR flip-flop are shown in Fig. 10 with the set and reset signal with 16 bit NRZ data at the data rate of 8.5 Gb/s. From Fig. 10, we can see that the output Q will maintain the previous state until a set or reset signal is set to logic 1. When set signal is set to 1, the Q output shows logic 1 and is maintained until the reset signal is logic 1. Similarly with reset signal set to 1, the output Q gives logic 0 until the set signal is 1 which proves the SR flip-flop. It is maintained that S and R never are at logic 1 state at the same

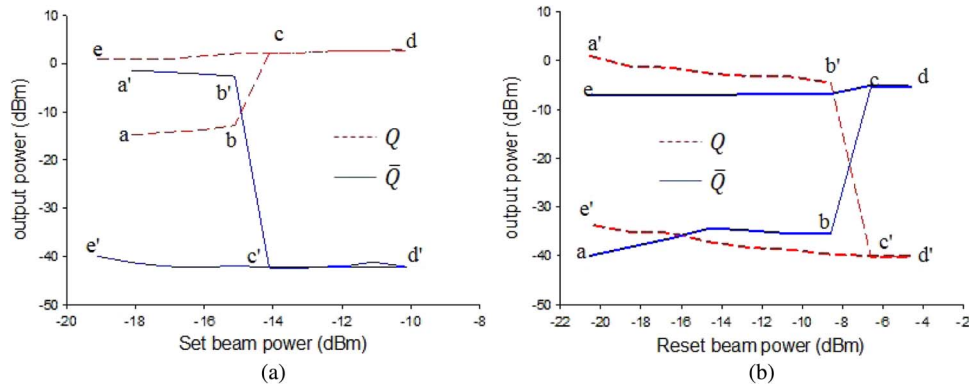


Fig. 9. Output power of  $Q$  and  $\bar{Q}$  with change in (a) set beam power (b) reset beam power.

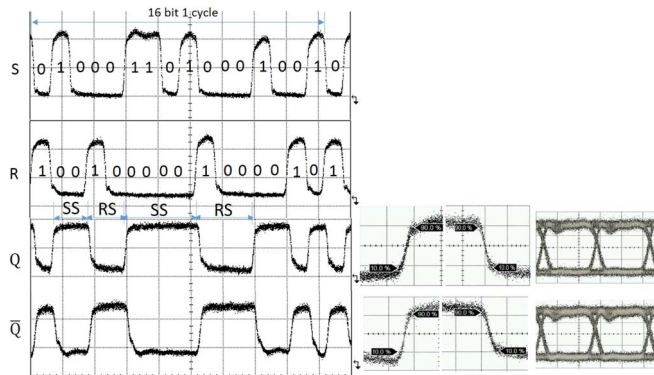


Fig. 10. Output waveforms, rising and falling time, and eye diagram of SR flip flop with 8.5 Gb/s NRZ signal with time scale of 200 ps/div, 100 ps/div, and 20 ps/div, respectively. SS: Set state and RS: Reset state.

time because it gives unspecified output. Outputs  $Q$  and  $\bar{Q}$  are always in opposite state in logic which gives two simultaneous inverted and non-inverted output of SR flip-flop. The rising and falling time of output  $Q$  is measured as 27.9 ps and 31.6 ps and that of  $\bar{Q}$  is measured as 33.2 ps and 40.9 ps, respectively. Pseudo random bit sequence (PRBS) signal with length of  $2^{31}-1$  is used to measure the eye diagram and BER. The extinction ratio of 14.08 dB and 12.96 dB is measured for  $Q$  and  $\bar{Q}$ , respectively. The BER plot in Fig. 11 shows no noise floor up to BER of  $10^{-12}$ . The maximum power penalty of 1.8 dB at the BER of  $10^{-9}$  is measured for  $\bar{Q}$ .

#### 4. Conclusion and Discussion

In this paper, we have demonstrated simultaneous inverted and non-inverted optical SR flip-flop based on SMFP-LDs with SR pulses at the data rate of 8.5 Gb/s and are verified with the spectrum domain results, output waveforms, rising/falling time, eye diagrams and BER results. We chose the power of set and rest signal as  $-14$  dBm and  $-6$  dBm, respectively which are modulated with different pulse duration to show that set and reset states remain on the same state even when the S and R signals are removed, until the S or R signal is set to logic 1. This proves the successful operation of the SR flip-flop. The main idea behind the SR flip-flop is the bistability characteristics on the injection locking of SMFP-LDs. The working speed of this S-R flip-flop is higher than that of our previous reported work with the speed of 1 Gb/s. Also, in this paper, we have shown the SR flip-flop with two simultaneous outputs and the analysis of the hysteresis loop width of bistability phenomenon with different wavelength detuning in SMFP-LD. We found that greater the wavelength detuning, the larger the hysteresis width, i.e., with high wavelength detuning, flip-flop can maintain

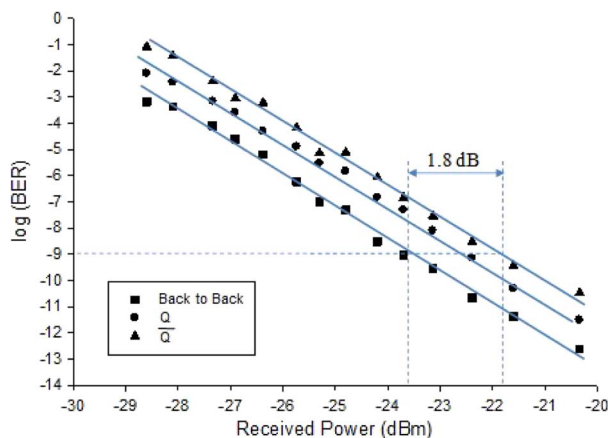


Fig. 11. BER and power penalty measurement for SR flip-flop.

the same state at the output with higher dynamic power range. However, increasing the wavelength detuning increases the power required for injection locking and suppressing of the dominant mode of SMFP-LD. Hence, the required power for set signal and reset signal is dependent on the wavelength detuning. The proposed and demonstrated simultaneous inverted and non-inverted SR flip-flop can be used for the latching circuits and also can be the step towards the short pulse based optical switch which does not need the control signal to be high throughout the operation as needed in the traditional optical switch. This type of switch can be useful for saving the power in the optical network. Since SMFP-LDs can work with various external beam wavelength pair, the SR flip flop can be used for the applications of Wavelength division multiplexing optical RAM and optical buffer in together with multi-wavelength access gate [23], [24] for the power, and cost effective solutions, which we have considered for the further research.

## References

- [1] F. Callegati, J. Aracil, and V. López, "Introduction," in *Enabling Optical Internet with Advanced Network Technologies*, J. Aracil and F. Callegati, Eds. London, U.K.: Springer-Verlag, Jan. 2009, pp. 1–4, ser. Computer Communications and Networks.
- [2] M. Hill *et al.*, "1 × 2 optical packet switch using all-optical header processing," *Electron. Lett.*, vol. 37, no. 12, pp. 774–775, Jun. 2001.
- [3] S. Zhang, Z. Li, Y. Liu, G. Khoe, and H. Dorren, "Optical shift register based on an optical flip-flop memory with a single active element," *Opt. Exp.*, vol. 13, no. 24, pp. 9708–9713, Nov. 2005.
- [4] J. Wang, G. Meloni, G. Berrettini, L. Poti, and A. Bogoni, "All-optical binary counter based on semiconductor optical amplifiers," *Opt. Lett.*, vol. 34, no. 22, pp. 3517–3519, Nov. 2009.
- [5] N. Pleros, D. Apostolopoulos, D. Petrantonakis, C. Stamatidis, and H. Avramopoulos, "Optical static RAM cell," *IEEE Photon. Technol. Lett.*, vol. 21, no. 2, pp. 73–75, Jan. 2009.
- [6] A. Kaplan, G. Agrawal, and D. Maywar, "Optical square-wave clock generation based on an all-optical flip-flop," *IEEE Photon. Technol. Lett.*, vol. 22, no. 7, pp. 489–491, Apr. 2010.
- [7] M. Hill *et al.*, "Integrated two-state AWG-based multiwavelength laser," *IEEE Photon. Technol. Lett.*, vol. 17, no. 5, pp. 956–958, May 2005.
- [8] Y. Liu *et al.*, "Packaged and hybrid integrated all-optical flip-flop memory," *Electron. Lett.*, vol. 42, no. 24, pp. 1399–1400, Nov. 2006.
- [9] H. Dorren *et al.*, "Optical packet switching and buffering by using all-optical signal processing methods," *J. Lightwave Technol.*, vol. 21, no. 1, pp. 2–12, Jan. 2003.
- [10] Y. Liu *et al.*, "All-optical flip-flop memory based on two coupled polarisation switches," *Electron. Lett.*, vol. 38, no. 16, pp. 904–906, Aug. 2002.
- [11] Y. D. Jeong, J. S. Cho, Y. H. Won, H. J. Lee, and H. Yoo, "All-optical flip-flop based on the bistability of injection locked Fabry–Perot laser diode," *Opt. Exp.*, vol. 14, no. 9, pp. 4058–4063, May 2006.
- [12] R. Clavero, F. Ramos, A. Martinez, and J. Marti, "All-optical flip-flop based on a single SOA-MZI," *IEEE Photon. Technol. Lett.*, vol. 17, no. 4, pp. 843–845, Apr. 2005.
- [13] M. Takenaka and Y. Nakano, "Realization of all-optical flip-flop using directionally coupled bistable laser diode," *IEEE Photon. Technol. Lett.*, vol. 16, no. 1, pp. 45–47, Jan. 2004.
- [14] K. Huybrechts, R. Baets, and G. Morthier, "All-optical flip-flop operation in a standard tunable DBR laser diode," *IEEE Photon. Technol. Lett.*, vol. 21, no. 24, pp. 1873–1875, Dec. 2009.

- [15] Y. Deok Jeong, Y. Hyub Won, S. Ook Choi, and J. Hyun Yoon, "Tunable single-mode Fabry–Perot laser diode using a built-in external cavity and its modulation characteristics," *Opt. Lett.*, vol. 31, no. 17, pp. 2586–2588, Sep. 2006.
- [16] D. M. Gvozdić, M. M. Krstić, and J. V. Crnjanski, "Switching time in optically bistable injection-locked semiconductor lasers," *Opt. Lett.*, vol. 36, no. 21, pp. 4200–4202, Nov. 2011.
- [17] M. Krstić, J. Crnjanski, and D. Gvozdić, "Injection power and detuning-dependent bistability in Fabry–Perot laser diodes," *IEEE J. Sel. Topics Quantum Electron.*, vol. 18, no. 2, pp. 826–833, Mar./Apr. 2012.
- [18] M. M. Krstić, J. V. Crnjanski, and D. M. Gvozdić, "Switching time and energy in bistable injection-locked semiconductor multi-quantum-well Fabry–Perot lasers," *Phys. Rev. A, At. Mol. Opt. Phys.*, vol. 88, no. 6, pp. 063826-1–063826-8, Dec. 2013.
- [19] J. S. Cho, N. L. Hoang, Y. D. Jeong, and Y. H. Won, "Optical bistability of an injection-locked single-mode Fabry–Perot laser diode and its application to an optical flip-flop," presented at the Conf. Lasers Electro-Optics/Pacific Rim, Seoul, Korea, Aug. 2007, Paper. ThP\_097.
- [20] E. Lau, H.-K. Sung, and M. Wu, "Frequency response enhancement of optical injection-locked lasers," *IEEE J. Quantum Electron.*, vol. 44, no. 1, pp. 90–99, Jan. 2008.
- [21] M. Krstić *et al.*, "Multivalued stability map of an injection-locked semiconductor laser," *IEEE J. Sel. Topics Quantum Electron.*, vol. 19, no. 4, p. 1501408, Jul./Aug. 2013.
- [22] H. Yoo, Y. D. Jeong, Y. H. Won, M. Kang, and H.-J. Lee, "All-optical wavelength conversion using absorption modulation of an injection-locked Fabry–Perot laser diode," *IEEE Photon. Technol. Lett.*, vol. 16, no. 2, pp. 536–538, Feb. 2004.
- [23] G. Kanellos *et al.*, "Bringing WDM into optical static RAM architectures," *J. Lightwave Technol.*, vol. 31, no. 6, pp. 988–995, Mar. 2013.
- [24] P. Maniotis, D. Fitsios, G. Kanellos, and N. Pleros, "Optical buffering for chip multiprocessors: A 16 GHz optical cache memory architecture," *J. Lightwave Technol.*, vol. 31, no. 24, pp. 4175–4191, Dec. 2013.